Microstructure and Wear Analysis of FeBCr Based Coating Deposited by HVOF Method

M.S. Priyan[a], P. Hariharan[a], A. Azad[a], K.S. Kumar[a]

[a] College of Engineering, Guindy, Anna University, Chennai-600025, Tamil Nadu, India.

Corresponding author:

M. Shunmuga Priyan
College of Engineering,
Anna University,
Chennai-600025,
Tamil Nadu, India.
Email: shunceg@gmail.com

A B S T R A C T

Thermally sprayed coatings that are based on FeBCr-related alloy powders are widely used to improve properties such as the surface hardness and wear resistance of a variety of coated metal substrate materials. Gray cast iron is widely used in the automobile industry due to its low cost and performance. In this work Gray cast iron substrate is coated with FeBCr alloy powder to improve its performance. The microstructure and micro abrasive wear performance of both the uncoated substrates and the coated substrates were characterized by optical microscopy as well as by Scanning Electron Microscope (SEM). In addition, X-ray Diffraction (XRD) was undertaken in the partial characterization of the coating. The densely layered coating had porosity levels that were below 2.5 % and a high surface hardness, of the order of 980 HV0.1. The coating exhibited excellent wear resistance when subjected to the ball-cratering test method. The low coefficients of friction of hard coating on the substrate were recorded. The wear performance of the coating was nearly 82 % better than that of the substrate, with a 0.05 N load, even under severe three body abrasive conditions.

1. INTRODUCTION

Gray iron is the workhorse of cast metals, offering versatility and low cost. Gray cast iron is used [1] widely in the manufacture of automotive components. It has good casting properties, good vibration damping, good wear resistance, good machinability and low notch sensitivity and, most importantly, lower production costs that alternative substrates. The mechanical and surface properties of gray cast iron can be improved by the use of thermal spray coating techniques, such as the HVOF method. Abrasive wear is significant to many industries. In many instances, it is more severe

in service than is anticipated, leading to the short life of components and/or hindrance to the further function of the components. Increasing the abrasive resistance of those components that are used in critical sliding situations through the use of suitably resilient and cost effective coatings has become the order of the day. In several contemporary industrial practices, thermal spraying is often considered as offering a potential alternative to traditional coating techniques such as hard chrome electroplating, for the production of wear resistance coatings. For instance, in the testing of piston rings that have been treated with different coatings, HVOF sprayed, chromium carbide coated piston rings

have been shown to give a better performance in wear testing and scuffing resistance than can be achieved with chromium plated piston rings, after heavy duty diesel engine testing [2]. A suitable iron compound-based alloy coating, by HVOF process, would be highly potential candidate for industrial and automotive application owing to their excellent wear resistance, high temperature stability, good magnetic properties, superior corrosion properties and importantly low material cost. In the recent past, in-depth studies have been done on the tribological properties of iron compound-based WC/12Co coatings [3] and also on iron-compound-based amorphous coatings incorporating compounds such as those of the general formula type, $Fe_{48}Cr_{15}Mo_{14}C_{15}B_6Y_2$ [4]. However, very little work has been published with respect to FeBCr-based coatings, including consideration of their wear performance and characteristics. The substrate material for this work was gray cast iron, as used for automobiles. Interestingly, micro-alloyed gray cast iron has been shown to improve significantly the abrasive wear resistance, with respect to the performance of "ordinary" gray cast iron, because of the presence of very hard phosphate ion-provided eutectics [5]. In the current study, a FeBCr coating was successfully deposited on a gray cast iron substrate by HVOF thermal spraying, under controlled conditions. In addition, the wear properties of the resulting coated substrates were studied.

The micro abrasion wear test, conducted using the block–on–ring method produces an imposed, wear-scar geometry [6-8]. In ball cratering, the wear depth increases at the same rate in both the coating and substrate [9]. The geometry of the wear scar is assumed to reproduce the spherical geometry of the rotating ball. Hence, the wear volume may be calculated by the measurement of either the crater diameter or its depth. Abrasive slurries such as those containing either (or both) SiC and Al_2O_3 have been widely used to evaluate different coatings. However, in this study, a diamond abrasive with a mean particle size of 4 μm was used as a suspension in distilled water. Variations of wear volume with respect to the slurry concentration were found to be nonlinear, exhibiting a maximum wear volume at 0.1 to 0.2 g/cm^3 when the SiC abrasive medium was used [6]. At low slurry loadings the wear volume was almost independent of loading

in the slurry, being dependent predominantly on the amount of slurry that was used [6]. To institute a severe abrasive condition, a relatively large amount of the abrasive medium was used in the slurry, of the order of 0.1 g/cm^3. Usually two abrasive wear modes are observed on the surface of the worn crater. These are rolling abrasion, which results when the abrasive particles roll on the specimen and grooving abrasion, which occurs when the abrasive particles slide on the specimen [10-13]. The type of wear mode that is operating has a significant effect on the wear rate of a tribologic system [14,15]. Previous research has revealed the gray iron is a relatively inexpensive and effective material for many applications. It differs from other forms of cast iron in that the excess carbon that was in solution, any amount beyond the saturation point of the metal, precipitates, in the form of graphite flakes that are imbedded within the matrix. This unique structure allows cast components readily to absorb vibration and to possess a self lubricating quality, giving excellent wear resistance [16]. Fe-based amorphous metallic glasses are considered to be extremely viable candidates as surface protective coatings owing to their high crystallization temperature, wear resistance, good magnetic properties, and relatively low material cost [17]. Micro structural studies have shown that the coatings present a dense layered structure, a low extent of porosity and low metal oxide content. Thus, all of the coatings have a low porosity, this being less than 2 %, a value that is typical of HVOF-sprayed coatings [18]. Using HVOF, dense/hard FeCrMoCBY-based coatings have been created, these having an almost fully amorphous structure. Such coatings exhibit wear resistance properties that are several times greater than those generated using electroplated Cr-based and Ni-based amorphous coatings [19]. Fe-based amorphous alloys are considered to be extremely visible candidates for surface protective coatings owing to their high crystallization temperature, their wear resistance, their good magnetic properties and the lower material costs [20]. Iron-based alloy powders produce products with very low hardness and reduced relative brittleness, the causes of which have been ascertained using various techniques, such as microstructural analysis [21,22]. Fe-based, amorphous metallic glasses are considered to be extremely viable candidates as surface protective coatings owing

to their high crystallization temperature, their superior corrosion and their wear resistance, coupled with their good magnetic properties and relatively low material costs [23-26]. The micro-structural characteristics of the amorphous coatings were investigated using several test methods. The micro-hardness, friction and wear behaviour of the coatings were also examined. This paper presents work undertaken in the production of FeBCr- based powders that were designed for use in thermal spraying. The powder feedstock and sprayed coatings have been micro-structurally characterised. The solid coatings were subjected to diamond slurry abrasive wear testing. In addition, the mechanisms of wear were determined by examination of the wear scars.

2. EXPERIMENTAL PROCEDURE

2.1 Material and Coating Preparation

The crystalline coatings, at 400 μm thickness were prepared using a Jet gun HVOF spraying system. The optimised spraying parameters are presented in Table 1.

Table 1. Chemical composition of the substrate and coating.

Sample No	Composition (%)	Fe Based alloy Powder
1	Fe	59
2	B	26
3	Cr	15

Sample No	Composition (%)	Gray Cast Iron
1	Fe	94.78
2	Cr	3.0
3	Si	1.320
4	B	0.283
5	Cr	0.0847
6	Mn	0.264
7	Ni	0.017
8	P	0.283

The atomized Fe-based alloy powders, with particle sizes in the range of 15-75 μm were used for spraying onto the gray cast-iron substrates. Powders of the same composition were produced by a high pressure argon gas atomization method. They were then sieved according to conventional sieve analysis, being subdivided into different size ranges. Gray cast iron was the desired choice of substrate material, being the most prevalently used material for those automotive applications in

which continuous abrasion and exposure to high temperature is undergone in its regular service. The chemical composition of the selected substrate material is provided in Table 2.

Table 2 – HVOF process parameters.

Sample No	Parameters	Qty
1	Gun type (Super jet Gun)	1 No
2	Pressure of Oxygen	2.5 kg/cm²
3	Pressure of acetylene	0.6 kg/cm²
4	Torch angle with respect to substrate	60°
5	Torch Speed	12 cm/min
6	Distance of torch tip from the substrate	25 mm
7	Preheat temperature	200 °C

Suitable specimens, (length 12 mm and diameter 24 mm), were fabricated from the substrate bar by EDM wire cutting to a close proximity to the required size, followed by the grinding of both the faces, to remove surface irregularities as well as to deal with the consequences of any induced micro-level changes that might have occurred in the heat affected zone as a result of the EDM cutting. The surface roughness of the samples was maintained at around 0.6 μm by the grinding operation. The raw material for the coating, namely the FeBCr alloy powder, was obtained from M/s L&T EWAC powders Ltd. This had a pre-mixed composition of Fe-59 %, B-26 % and Cr-15 %. The presence of Cr alloys improves the wear properties, the thermal stability and the corrosion properties of coating. The atomized powder particles were in the size range of 40 to 80 μm. An appropriate HVOF system was used for spray coating the powder on the substrate specimen, this having been previously thoroughly cleaned with acetone and subsequently dried. The spraying parameters were optimized so as to produce a coating layer of about 400 μm thickness, details of which are presented in Table 1.

2.2 Coating Characterization Methods

Samples from the surfaces of the coatings and from cross sections of the coatings were polished using a series of coarser to finer grades of silicon carbide emery papers and then finally polished with a diamond paste, applied on a velvet cloth that was attached to a rotating disc. In this way, micro-polished surfaces were obtained for further analysis and evaluation. The

sample was etched with Nital to reveal microstructural features of interest, Fig. 1, Scanning Electron Microscopy (SEM) image analysis was used to quantify the distribution of different phases in the samples of interest.
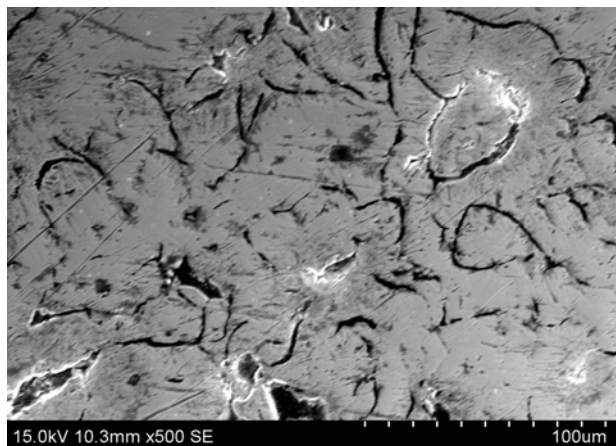

Fig. 1. SEM images of coated Specimen etched with Nital.

Optical microscopy was used to calculate porosity level by image analysis. The coating thickness values were determined by the SEM technique using the cross sectioned samples. A stereographic image analysis system was employed to estimate the average porosity (%) of the coated surface, by analyzing and averaging various optical micrographs that were taken at different surface regions of the coating, as outlined in the standard test method, ASTM B276. To give a guide to the weight percentage of particular elements and atoms, EDAX was used at random locations on the coating surface. Also X-Ray Diffraction (XRD) patterns were used to characterize the coating type. This XRD analysis of the specimens was performed on an X-ray diffractometer (Cu K_α radiation) with a range of 2θ diffraction angles from 40 to 50°. The micro-hardness value was determined for the uncoated specimens and for the coated specimens. The micro-hardness was tested at various places on the coating surface using Wolpert Wilson equipment, model 402 MVD. A load of 1 N (100 g) was employed for a dwell time of 10 seconds.

2.3. Wear test and evaluation

Wear performance of the coating was the bare substrate was assessed by a micro abrasion test in which the samples were subjected to a block-on-ring method of testing with diamond slurry as abrasive medium to increase the severity of the abrasion. A commercially available Wear and friction unit from Tech (India) Pvt. Ltd. (Fig. 2), was used for the test, in accordance with the standard ASTM G 77 procedures, in which the coated samples were pressed against a directly driven steel ball, under a fixed load, rotating at 150 revs/minute corresponding to a linear sliding distance of 11.78 m.
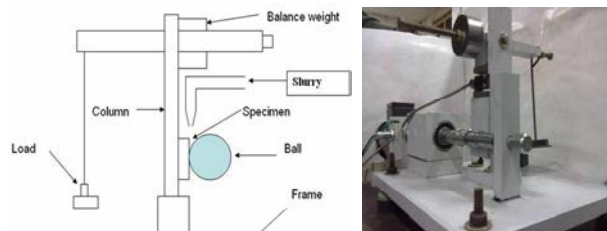

Fig. 2. Schematic diagram of micro abrasion tester.

The test sample was clamped onto a platform, fitted to the pivoted L-shaped arm. This arm was rotated around its pivot until the sample came in contact with the ball. The beam was balanced when the samples were in contact and the load was applied by adding dead weights to a cantilever arm. This configuration has the advantage of providing accurate control of both the normal load and the sliding speed. Furthermore, the coating was subjected to abrasion testing using three different loads, namely 0.05, 0.1, and 0.2 N, for durations of 2, 4, and 6 minutes for each of these loads. Diamond powder-based slurry was continuously fed in to the interface between the ball and sample throughout the tests. The complete test parameters are presented in Table 3.

Table 3. Micro-abrasion test parameters.

Substrate	Fe based alloy coated specimen, Surface roughness Ra=0.6μm.
Ball material	High Carbon – High Chromium material conforming to EN 31 Ball d iameter-25.4 mm, Surface roughness Ra=0.068 μm. Hardness-750 VHN at 100 g load
Sliding distance	11.78 m
Load	0.05, 0.1 and 0.2 N
Test Duration	2, 4, 6 minutes
Slurry	Diamond slurry with distilled water, Particle size (<1μm) triangular shape

An instantaneous plot for the coefficient of friction versus the time was obtained through the use of compatible software, as the test progressed. The wear coefficients for the

coating, (kc), and for the substrate, (ks), were noted from these plots and the results compared. The wear volume (V) was calculated from the crater diameter of wear scar, using video imaging, by the formula: $V = \pi d^4/64R$. Here, d is the diameter of the wear crater and R is the radius of the spherical ball. The Archard wear law states that the volume of wear $V = KSN$, where K is a constant (the wear rate), S is the sliding distance and N is the applied load. This relationship has often been found to be appropriate. However, in some cases, a strong dependence of the wear rate on the number of revolutions and hence on the sliding distance has been found. The resultant wear scars were in the shape of a spherical crater, the geometry of which corresponded to that of the spherical ball used in wear test. The extent of wear damage was quantified in terms of surface roughness and the wear volume of the resultant scars.

3. RESULTS AND DISCUSSION

3.1. Coating characterization

Usually, pre-alloyed feed stock powders are deposited on the substrate material by thermal spray coating. Figure 3 represents the SEM image of the Fe-59 %, B-26 % and Cr-15 % feedstock powders. The diameters of the particle are in the range from 25–45 μm. The majority of the particles that were produced by gas atomization in argon atmosphere are spherical or near-spherical although some have small satellites attached. Most of the particles exhibit a smooth surface, this being the source of the good fluidity of the system. On the impact of the high temperature molten droplets, localized melting of the substrate takes place, creating a metallic bonding between coating and substrate. If necessary the substrates can be grit blasted to improve the adhesion of coating. The bonding strength that develops between the substrate and the coating is the major factor in determining the strength of the adhesion. This study was aimed at establishing the wear resistance of coating, even when the coating was applied over a smooth substrate surface. For this purpose, the substrate surface was ground to a 0.6 μm surface roughness prior to coating. The microstructure of the surfaces and the cross sections are identical, as shown in Fig. 4, and is replete with uniformly distributed fine grains,

presented as powder deposits with prominent wide boundaries, suggesting that a consistent coating was deposited through the use of the HVOF process.
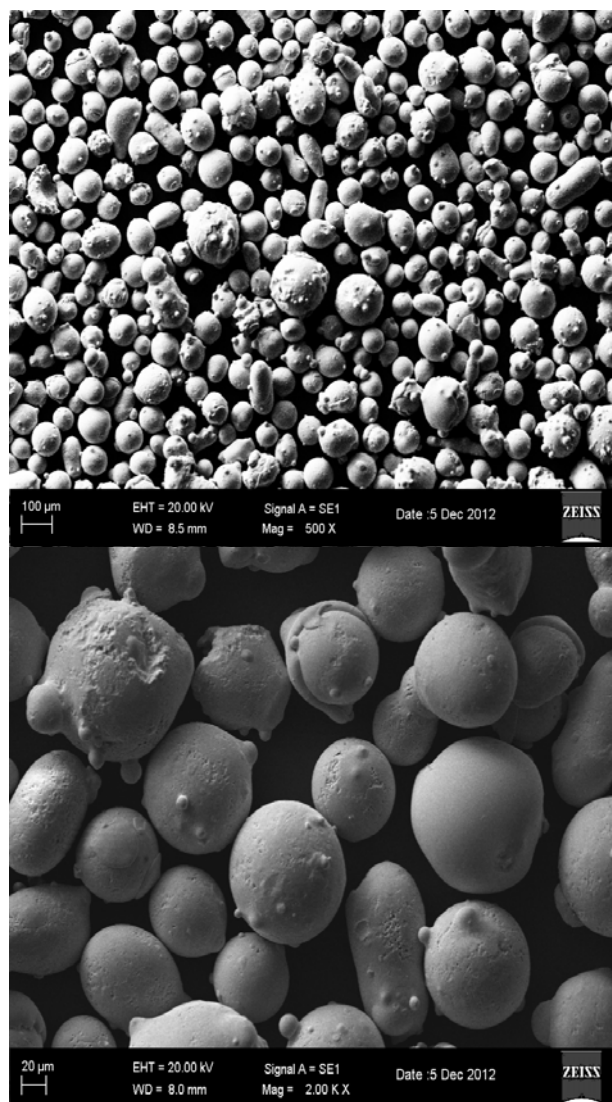

Fig. 3. As-atomized Fe based amorphous powder with particle size between 15-75 μm.
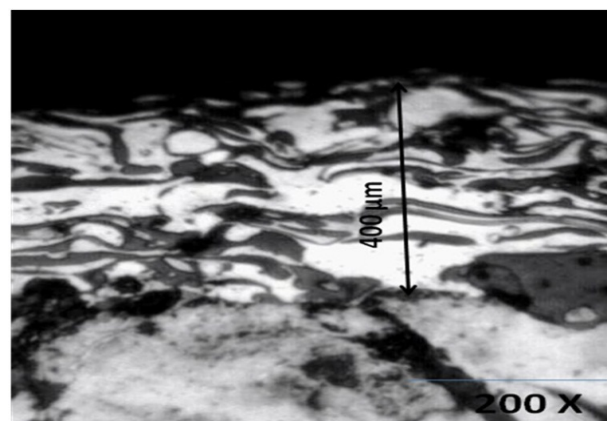

Fig. 4. SEM image of the cross section sample showing coating and substrate.

The SEM study of the cross sections of samples suggests that a consistent coating with an average coating thickness of 450 µm was created. The molten powders that impinge on the substrate have become flattened and solidified separately into blocks that are evenly distributed and, at the same time, are randomly laid over one another, leaving numerous gaps and separations in between the blocks. Despite this coating anomaly, which is an inherent feature, the overall porosity is less than 1.5 % and, moreover, the same level of porosity persists throughout the coating, signifying that effective/good deposition was achieved through the use of better process control. The formation of a dense coating is attributed to the high velocity of impingement, a characteristic of the HVOF process. From the EDAX analysis, as shown in Fig. 5, the predominant Fe peak and Fe-B-Cr peaks are indicative of the fact that these are the major atomic % constituents of the matrix.
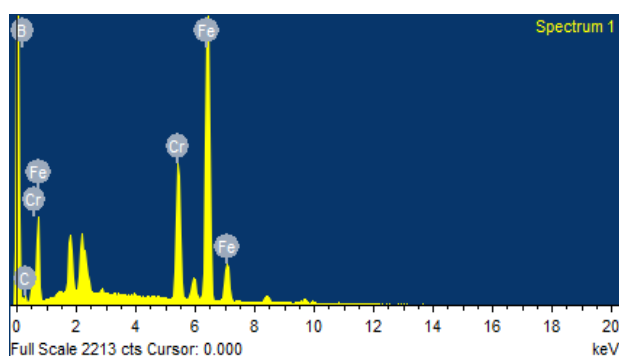

Fig. 5. EDX analysis of coating.

The image shows that there is no trace of oxygen on the coating surface, showing the surface of the coating to be devoid of metal oxide species.

3.2. Surface morphology of the coating

Figure 6 represents an optical micrograph of the top surface of the coating. It shows the presence of a nearly uniformly distributed, fine-grained microstructure. A typical region from a cross-section of the coating reveals its dense layered structure, as shown in Fig. 4, although some pores exist as very dark regions as can be seen in the images. In general, the big pores that are located between the flattened droplets are mainly caused by the loose packed layer structure or by some gas porosity phenomenon, while the small pores within the flattened particles originate from porosity that develops during shrinkage [28]. In spite of the presence of these defects, the coatings show a level of porosity that is below 1.5 %, which is typical of HVOF-thermally sprayed deposits. Also, it can be seen that a gradient in porosity exists across the thickness of the coatings, i.e., the top layers seem to be the more porous and have more interfaces than the rest of the coating.
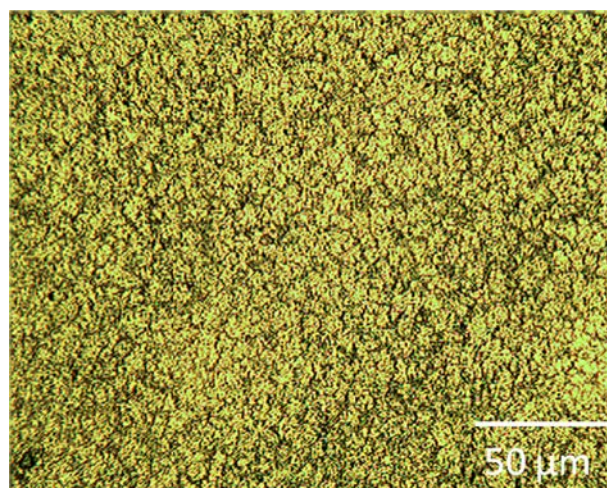

Fig. 6. Optical micrographs showing surface morphology of HVOF sprayed Fe based alloy coating on gray cast-iron.

This micro structural characteristic may be significantly affected by the newly incoming particles with their high velocity opening the previously deposited layers [29].

3.3. Micro hardness of the coating

A micro hardness profile, along the cross section of the coating, as a function of distance from the coating–substrate interface, is shown in Fig. 7, from which it can be inferred that there was a gradual increase of hardness from the interface towards the coating surface.
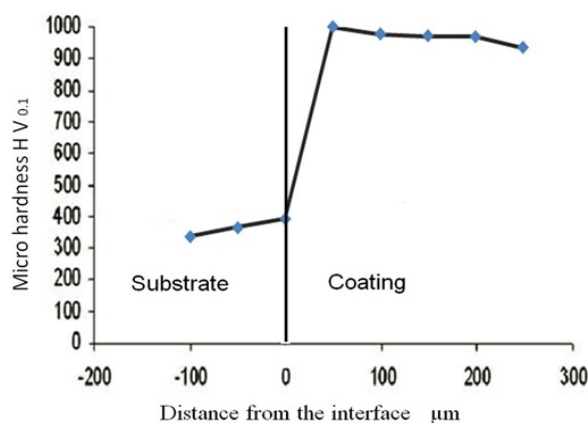

Fig. 7. Micro hardness profile for HVOF sprayed Fe based alloy coating.

The average surface hardness of coating was 920 HV0.1, about twice that of the substrate hardness which is around 350 to 400 HV. Towards the interface the coating hardness is around 750 HV0.1 and at a distance of 250 microns above the interface the hardness reaches a maximum level of about 910 HV0.1 and remains stabilized with respect to the surface at 450 microns away from interface. This stabilized hardness is of great significance as it enhances the wear resistance capabilities of the coating compared to the wear resistance that can be achieved in a system of gradient hardness. The greater hardness of the coating is attributed to solid-solution strengthening by the B and the Cr in Fe phase.

The XRD patterns of the atomized powder, as the substrate material and as a deposited coating are shown in Fig. 8. This figure confirms the coating to be predominantly of a crystalline nature, as seen in the sharp peak corresponding to the α phase, at 2θ, of 45 deg.
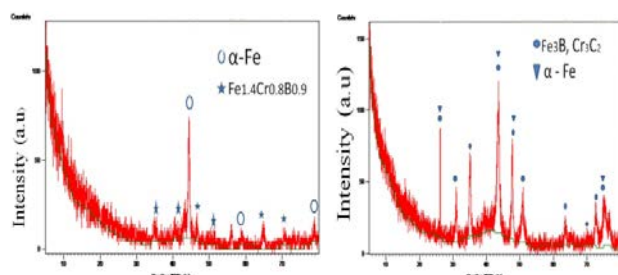

Fig. 8. XRD pattern of FeBCr Powder and FeBCr Coated Surface.

The SEM image of the feedstock powders of the coatings is shown in the inset of Fig. 3.The image shows that majority of the particles, which were prepared by gas atomisation under argon atmosphere, are spherical, although some have small satellites attached to them. The XRD patterns show a broad halo peak at 2θ=40–50°, which overlaps to a small extent with the peaks relating to crystalline diffraction. With the FeB alloy, the XRD patterns showed that coating structure are more crystalline than is the structure of powder and that the cubic structure of Fe_3B is the principal characteristic of the FeB alloy, Fig. 8. These results are similar to those obtained by the rapid quenching of FeB mechanically produced alloys [23]. The diffraction pattern confirms the BCC structure of the α-Fe matrix. It is worth noting the emergence of a broad halo between the 2θ values of approximately 40° and 60°. These are related to the formation of an amorphous phase [27].

3.4. Wear Mechanisms

In an attempt to establish the characteristics of the wear behavior of the coatings, the worn surfaces were examined by Video image. The wear scar nature of the tested coatings, Fig. 9, shows abrasive marks, pits and excess wear debris, indicating that three-body abrasive wear was the dominant wear mechanism.
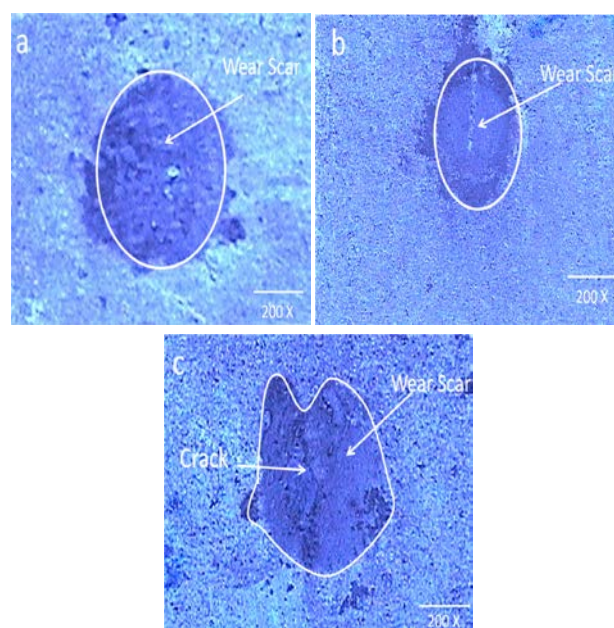

Fig. 9. (a) A_g/A_p ratio as a function of the test time, for ball material and Coated surface; (b) Rolling abrasion, for the condition $A_g/A_p=0$; and (c) rolling and grooving abrasion, for the condition $0<A_g/A_p<1$.

However, in addition, fine wear-tracks are observed uniformly all over the scar. Also, a few deep grooves are present, possibly formed due to the occurrence of ploughing during the test, caused by isolated and accumulated abrasive diamond particles. Under hard abrasion conditions, abrasive particles can cause plastic deformation in both the hard particles and the binder phase. The contact area for individual abrasive particles is usually much larger than that of the surface particle, and wear occurs predominantly by plastic ploughing and cutting. Figure 10 shows the global distribution of wear debris. Signs of "adhesive wear" are also evident along the wear-tracks. In an attempt to identify the wear mechanisms taking place in the different conditions, the worn surfaces were examined by SEM. In the case of the diamond slurry, and for deposited coatings, the craters

produced by the diamond suspension show deep parallel scratches, with plastically deformed edges, caused by the hard diamond abrasive particles (Fig. 10).
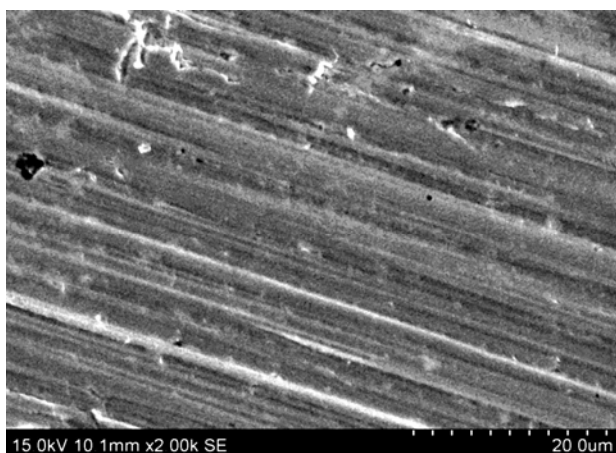

Fig. 10. Wear grooving morphology of coated surface at loading condition.

This process occurs when a significant proportion of the slurry particles are embedded in the surface of the ball and act as fixed indenters, causing the two body abrasion (or grooving) wear mode. The worn surfaces of Fe based alloy coated specimens from rotating ball as well as unidirectional grooving and rolling tests were analyzed by using SEM. The micro cutting action is clearly evident in the coated specimen. Further, the micro cutting is accompanied by significant micro-ploughing action. The cracking of material at the wear groove edges can be clearly seen. An optical microscopy analysis of the wear craters obtained in this work indicated that, in all cases, the abrasive wear mode was grooving abrasion: a condition that may be defined as the ratio of grooving area (A_g) to projected area (A_p) is normalized equal to 1 ($A_g/A_p = 1$). However, when a more detailed analysis was conducted with the help of a SEM, the occurrence of rolling abrasion was observed alongside the grooving abrasion, i.e, the SEM revealed the occurrence of rolling abrasion along the grooves.

The friction coefficient of the amorphous coatings and of the gray cast iron substrates, related to testing time, was monitored (Fig. 11). However, under the different conditions, the coating demonstrated a significantly greater coefficient of friction than that pertaining to the substrate material. Appreciably severe abrasive particles, such as diamond, lead to 'severe' abrasion.
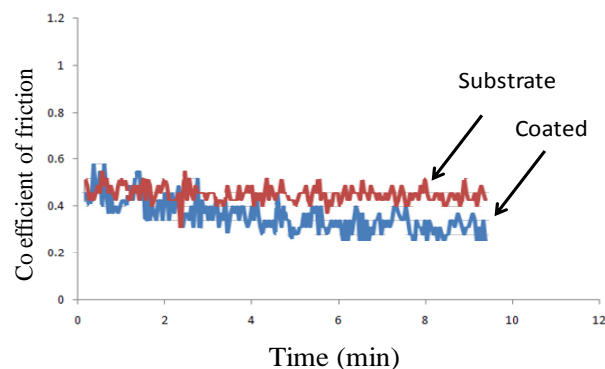

Fig. 11. Online monitoring of coefficient of friction for coating & substrate.
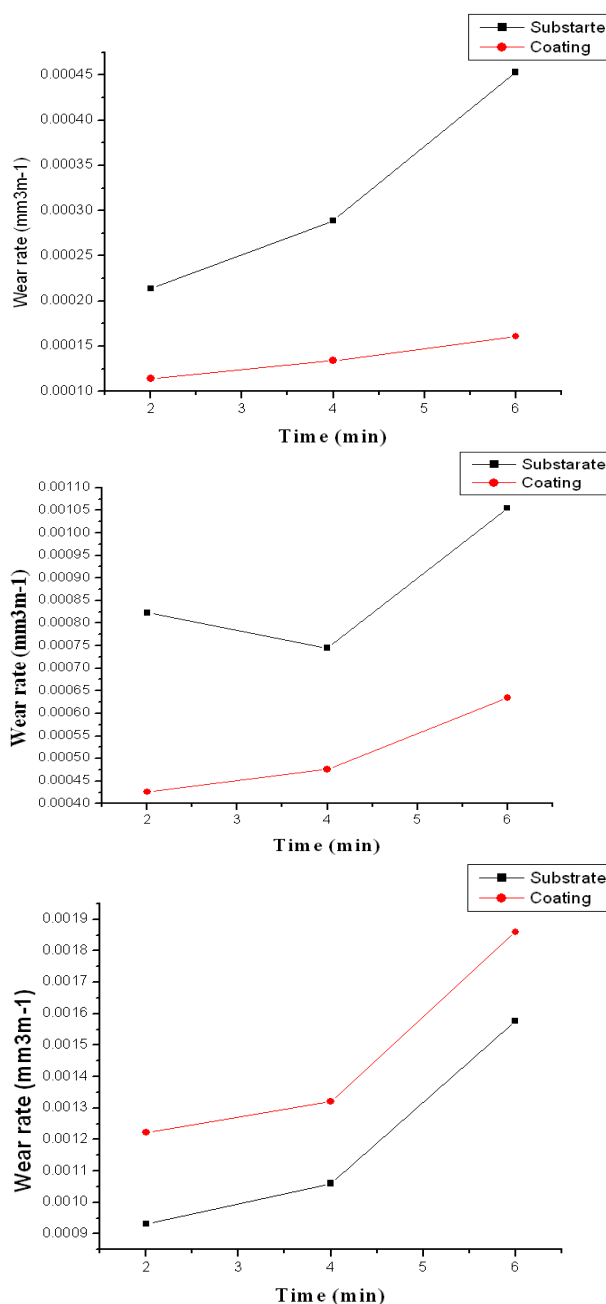

Fig. 12. Wear rate monitoring of coated and un-coated surface at different conditions (a) 0.05 N; (b) 0.1 N; (c) 0.2 N.

Practical bearing surfaces often deteriorate with time as a result of hard particulate contaminants being swept through the clearance gap. These particles may arise from the external environment or be wear debris from other pairs of surfaces. The mechanics of surface damage in such circumstances has been examined both experimentally and analytically [30]. Another way of judging the wear performance is to compare the extent of material removal in terms of wear volume, in both the coating and the substrate. From the direct plot of the wear rate and the test time, Fig. 12, it is apparent that the volume of wear increases as the applied load increases and as the testing duration increases. As expected, under each load condition, the coating exhibits comparatively less wear than the substrate.

Interestingly, Fig. 12 shows that the wear performance of the coating is nearly 82 % greater than that of the substrate, at a 0.05 N applied load. However, at the greater applied loads of 0.1 N and 0.2 N, the wear performance of the coating declines drastically, being only slightly better, by about 20 % and 15 % respectively, than the wear performance of the substrate. This indicates that the diamond abrasive played a major role in the wear that took place in testing, irrespective of change in the characteristic behavior of the subsurface at higher loads. Thus, above the 0.05 N load, the coating performs with consistently less wear resistance.

4. CONCLUSION

In this study, an attempt was made to develop an amorphous coating of an iron complex-based alloy. F_eBC_r coatings were successfully deposited on Gray cast iron by the HVOF spraying process to develop coatings of 350 to 400 μm in thickness. The HVOF-sprayed coatings, with given parameters, have dense and uniform lamellar microstructures with porosities of less than 1.5 %. Further, a high proportion of the feedstock powders appeared to have been fully or partiality melted prior to impact on the substrate surface. The SEM micrographs indicate that the coatings are free from surface/cross-sectional crack defects. X-ray diffractograms indicate that F_e-59 %, B-26 % and C_r-15 % powder alloy coatings have an iron-based bcc structure as a principal phase. EDAX analysis of the as-sprayed coatings has indicated the formation of the required compositions of the coatings. The iron-based alloy coatings have shown maximal hardness in the range of 800 to 900 HV. The micro-hardness of the coatings is greater than that of the substarte. Furthermore, the micro-hardness of the coatings varies with the thickness of the coating. The wear rate performance coating is nearly 82 % greater than that of the substrate, at 0.05 N applied load.

REFERENCES

[1] *Automotive Gray cast iron Castings HS-30/2000.Div 9 Automotive iron and steel castings, SAE standards, August 1996.*

[2] M. Shuster, F. Mahler, D. Crysler: *Metallurgical and Metrological Examinations of the Cylinder Liner-Piston Ring Surfaces After Heavy Duty Diesel Engine Testing,* Tribology Transactions, Vol. 42, No. 1, pp. 116 – 125, 1999.

[3] Terajima Takeshi, Takeuchi Fumiya, Nakata Kazuhiro, Adachi Shinichiro, Nakashima Koji, Igarshi Takanori: *Tribological properties of WC/12Co Cermet -Fe- Based metallic glass spray coating,* Transactions of JWRI, Vol. 38, No.1, 2009.

[4] Z. Zhou, L. Wang, D.Y. He, F.C. Wang, Y.B. Liu: *Microstructure and wear resistance of Fe based amorphous metallic coatings prepared by HVOF thermal spraying*, Journal of Thermal Spray Technology, Vol. 19, No. 6, pp. 1287-1293, 2010.

[5] J. Keller, V.F Ri Drici, P.H. Kapsa, S. Vidaller, J.F Huard: *Influence of Material Nature and Surface Texturing on Wear of Heavy-Duty Diesel Engine Cylinder Liners*, Tribology Transactions, Vol. 52, pp. 121-126, 2009.

[6] R.I. Trezona, D.N. Allsopp, I.M. Hutchings: *Transitions between two body and three-body abrasive wear: influence of test conditions in the micro scale abrasive wear test*, Wear, Vol. 225-229, No. 1, pp. 205-214, 1999.

[7] K.L. Rutherford, I.M. Hutchings: *Theory and application of a micro-scale abrasive wear test,* J. Testing and Evaluation. JTEVA, Vol. 25, No. 2, pp. 250-260, 1997.

[8] K.L. Rutherford. I.M. Hutchings: *A micro-abrasive wear test, with particular application to coated systems*, Surface and Coating Technology, Vol. 79 No. 1-3, pp. 231-239, 1996.

[9] A. Ramalho: *Micro-scale abrasive wear coated surfaces-prediction models*, Surface and coating technology, Vol. 197, No. 2-3, pp. 358-366, 2005.

[10] R.C. Cozza, D.K. Tanaka, R.M. Souza: *Friction coefficient and abrasive wear modes in ball-cratering tests conducted at constant normal force and contact pressure-Preliminary results*, Wear, Vol. 267, No. 1-4, pp. 61-70, 2009.

[11] K. Adachi, I.M. Hutchings: *Wear-mode mapping for the micro-scale abrasion test*, Wear, Vol. 255, No. 1-6, pp. 23-29. 2003.

[12] K. Adachi, I.M. Hutchings: *Sensitivity of wear rates in the micro scale abrasion test to test conditions and material hardness*, Wear, Vol. 258, No. 1-4, pp. 318-321 2005.

[13] K. Bose, R.J.K. Wood: *Optimum tests conditions for attaining uniform rolling abrasion in ball cratering tests on hard coatings,* Wear, Vol. 258, No. 1-4, pp. 322-332, 2005.

[14] R.C. Cozza, J.D.B. de Mello, D.K. Tanaka, R.M. Souza: *Relationship between test severity and wear mode transition in micro-abrasive wear tests,* Wear, Vol. 263, No. 1-6, pp. 111-116, 2007.

[15] Y.J. Mergler, A.J. Huis in 't Veld: *Micro abrasive wear of semi-crystalline polymers,* Tribol. Res. Design Eng. Syst, Vol. 41, pp. 165-173, 2003.

[16] C.R. Loper, R.W. Heine: *Ductile Iron Solidification Study Using Electron Microscope,* Transation of the A.F.S., Vol. 70, pp. 963-967, 1962.

[17] A. Inoue, B. Shen, C.T. Chang: *Super-high strength of over 4000 MPa for Fe-based bulk glassy alloys in* $(Fe_{1-x}Co_x)_{0.75}B_{0.2}Si_{0.05}]_{96}Nb_4$ *system,* Acta Materialia, Vol. 52, No. 14, pp. 4093-4099, 2004.

[18] J. Koutsky, J. Veselá: *Evaluation of white metal adhesion (conventional casting and thermal wire arc spraying) by ultrasonic non-destructive method*, J. Mater. Process. Technology, Vol. 157-158, pp. 724-728, 2004.

[19] X.Q. Liu, Y.G. Zheng, X.C. Chang, W.L. Hou, J.Q. Wang, Z. Tang, A. Burgess: *Microstructure and properties of Fe-based amorphous metallic coating produced by high velocity axial plasma spraying,* J. Alloys Compd., Vol. 484, No. 1-2, pp. 300-307, 2009.

[20] Hyung-Jun Kim, Stephanie Grossi, Young-Gak Kweon: *Wear performance of metamorphic alloy coatings,* Wear, Vol. 232, No. 1, pp. 51–60, 1999.

[21] O.C. Brandt, S. Siegmann, H.-P. Isch: *HVOF- and VPS-Coatings Using Nanostructured Iron-Based Alloys*. Conference proceedings. *1st United Thermal Spray Conference - Thermal Spray: A United Forum for Scientific and Technological Advances,* Indianapolis, Indiana, ISBN/ISSN: 0-87170-618-0, pp. 875-876, 1997.

[22] M. Cherigui, N.E. Fenineche, C. Coddet: *Structural study of iron-based microstructured and nanostructured powders sprayed by HVOF thermal spraying,* Surface & Coatings Technology, Vol. 192, No. 1, pp. 19 – 26, 2005.

[23] M. Abdellaoui, C. Djega-Mariadassou, E. Gaffet: *Structural study of Fe-Si nanostructured materials,* J. of Alloys and Compounds, Vol. 259, No. 1-2, pp. 241-248, 1997.

[24] S.J. Pang, T. Zhang, K. Asami, A. Inoue: *Bulk glassy Fe–Cr–Mo–C–B alloys with high corrosion resistance,* Corros. Sci., Vol. 44, No. 8, pp. 1847, 2002.

[25] S.J. Pang, T. Zhang, K. Asami, A. Inoue: *Synthesis of Fe–Cr–Mo–C–B–P bulk metallic glasses with high corrosion resistance,* Acta Materialia, Vol. 50, No. 3, pp. 489-497, 2002.

[26] A. Inoue, A. Makino, T. Mizushima: *Ferromagnetic bulk glassy alloys,* J. Magn. Magn. Mater., Vol. 215–216, pp. 246-252, 2000.

[27] C. Moreau, P. Cielo, M. Lamontagne, S. Dallaire, J.C. Krapez, M. Vardelle: *Temperature evolution of plasma-sprayed niobium particles impacting on a substrate,* Surface and Coating Technology, Vol. 46, No. 2, pp. 173-187, 1991.

[28] V.V. Sobolev, J.M. Guilemany: *Investigation of Coating Porosity Formation During High Velocity Oxy-Fuel (HVOF) Spraying*, Mater. Lett., Vol. 18, No. 5-6, pp. 304-308, 1994.

[29] T.C. Totemeier: *Effect of High-Velocity Oxygen-Fuel Thermal Spraying on the Physical and Mechanical Properties of Type 316 Stainless Steel,* J. Therm. Spray Technol., Vol. 14, No. 3, pp. 369-372, 2005.

[30] J.A. Williams, A.M. Hyncica: *Mechanisms of abrasive wear in lubricated contacts,* Wear, Vol. 152, No. 1, pp. 57-74, 1992.